ACS APPLIED MATERIALS & INTERFACES

Research Article

www.acsami.org

High-Performance Bottom-Contact Organic Thin-Film Transistors Based on Benzo[*d*,*d*′]thieno[3,2-*b*;4,5-*b*′]dithiophenes (BTDTs) Derivatives

Peng-Yi Huang,[†,‡] Liang-Hsiang Chen,[§,‡] Choongik Kim,[*,⊥] Hsiu-Chieh Chang,[†] You-jhih Liang,[†] Chieh-Yuan Feng,[†] Chia-Ming Yeh,[†] Jia-Chong Ho,[§] Cheng-Chung Lee,[§] and Ming-Chou Chen[*,†]

[†]Department of Chemistry, National Central University, Chung-Li, Taiwan, 32054, ROC

[§]Process Technology Division, Display Technology Center, Industrial Technology Research Institute, Hsinchu, Taiwan, ROC.

[⊥]Department of Chemical & Biomolecular Engineering, Sogang University, 1 Shinsoo-Dong, Mapo-Gu, Seoul 121-742, Republic of Korea.

Supporting Information

ABSTRACT: Three benzo[*d*,*d*′]thieno[3,2-*b*;4,5-*b*′]dithiophene (**BTDT**) derivatives, end-functionalized with benzothiophenyl (**BT-BTDT**; **2**), benzothieno[3,2-b]thiophenyl (**BTT-BTDT**; **3**), and benzo[*d*,*d*′]thieno[3,2-*b*;4,5-*b*′]dithiophenyl (**BBTDT**; **4**), were prepared for bottom-contact/bottom-gate organic thin-film transistors (OTFTs). An improved one-pot [2 + 1 + 1] synthetic method of **BTDT** with improved synthetic yield was achieved, which enabled the efficient realization of new **BTDT**-based semiconductors. All of the **BTDT** compounds exhibited high performance p-channel characteristics with carrier mobilities as high as 0.34 $cm^2/(V\ s)$ and a current on/off ratio of 1×10^7, as well as enhanced ambient stability. The device characteristics have been correlated with the film morphologies and microstructures of the corresponding compounds.

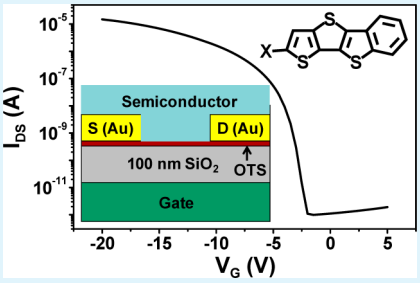

KEYWORDS: *benzothienodithiophene (BTDT), organic thin-film transistor (OTFT), organic semiconductor, bottom-contact, mobility, film morphology*

1. INTRODUCTION

Organic semiconductors have received significant interest over the past few decades as active components for the development of flexible electronic devices such as organic thin-film transistors (OTFTs).[1,2] Because of their unique properties compared to conventional inorganic materials, OTFTs are expected to be employed in a variety of applications such as flexible displays, printable RFID tags, and flexible solar panels.[3] Because the electrical properties of organic semiconductors are highly dependent upon their chemical structure,[4] the design, synthesis, and characterization of new organic semiconductors is of great interest.[5] Among organic semiconductors, pentacene, oligophiophene, and anthradithiophene derivatives are representative examples with high electrical performance.[6] In particular, fused thiophene derivatives with extensive molecular conjugation are of great interest due to their high carrier mobility and ambient stability.[7−12] For example, several fused thiophene derivatives have been reported with decent carrier mobilities (Figure 1). Considering p-channel fused thiophene-based semiconductors, **DP-DTT** (**A**),[7a,8] **DP-TTA** (**B**),[7b] **DBTDT** (**C**),[7c] and **BTBT** (**D**)[9] exhibited carrier mobilities of up to 0.42, 0.14, 0.51, and >1.0 $cm^2/(V\ s)$, respectively. For n-channel semiconductors,[10] we have reported **DFP-DTT** (**E**)[10b] and **DFP-TTA** (**F**)[10c] with electron mobilities as high as 0.07 and 0.3 $cm^2/(V\ s)$, respectively. Recently, a new series of fused thiophene derivatives based on benzo[*d*,*d*′]thieno[3,2-*b*;4,5-*b*′]dithiophene (**BTDT**) has been explored, and the phenyl end-capped derivative (**P-BTDT**; **1**) exhibited excellent electrical performance with a hole mobility of up to 0.70 $cm^2/(V\ s)$.[11] Furthermore, good electrical performance has been reported in optimized **DTBTE**-based (**G**) organic thin-film transistors (OTFTs), where a mobility of 0.50 $cm^2/(V\ s)$ was achieved, as compared to <0.01 $cm^2/(V\ s)$ in unoptimized **DTBT** (**H**).[12]

In this report, we investigate semiconductors based on fused thiophene, benzo[*d*,*d*′]thieno[3,2-*b*;4,5-*b*′]dithiophene (**BTDT**). We developed a new, simple synthetic methodology for the preparation of the **BTDT** core. Molecular structure−property relationships were elucidated by introducing benzothiophenyl (**BT-BTDT**; **2**), benzothieno[3,2-b]thiophenyl (**BTT-BTDT**; **3**), and benzo[*d*,*d*′]thieno[3,2-*b*;4,5-*b*′]-dithiophenyl (**BBTDT**; **4**) on the **BTDT** core, as shown in Figure 2. The developed semiconductor films were then employed as an active component in a bottom-contact/bottom-gate OTFT and the resulting device characteristics were investigated. Finally, the morphology and microstructure of

Received: October 7, 2012
Accepted: November 27, 2012
Published: December 6, 2012

   dx.doi.org/10.1021/am3022448 | *ACS Appl. Mater. Interfaces* 2012, 4, 6992−6998

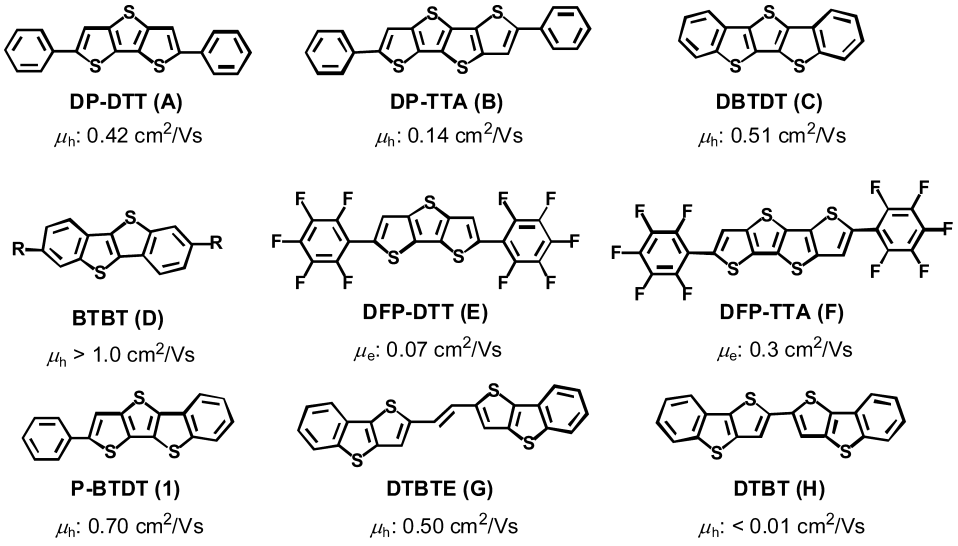

Figure 1. Examples of fused oligothiophene semiconductors used in OTFTs.

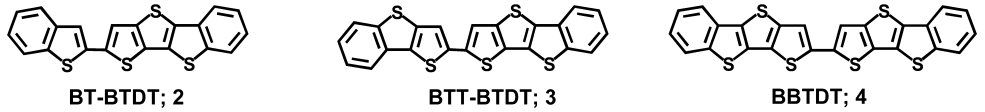

Figure 2. Chemical structures of the benzo[*d,d′*]thieno[3,2-*b*;4,5-*b′*]dithiophene (**BTDT; 2 - 4**) derivatives employed in this study.

the semiconducting films relating to film growth conditions were investigated to correlate these properties with device performance. In particular, bisbenzo[*d,d′*]thieno[3,2-*b*;4,5-*b′*]-dithiophene (**BBTDT**; **4**) exhibited excellent electrical performance with a carrier mobility as high as 0.34 cm^2/(V s) and a current on/off ratio of 1×10^7.

2. EXPERIMENTAL SECTION

2.1. Materials and Methods. All chemicals and solvents (from Aldrich, Arco, or TCI Chemical Co.) were of reagent grade. Reaction solvents (toluene, ether, and THF) were distilled under nitrogen from sodium/benzophenone ketyl, and halogenated solvents were distilled from CaH_2. ^{1}H and ^{13}C NMR spectra were recorded using a Bruker 500 or 300 instrument, with reference to solvent signals. Differential scanning calorimetry (DSC) was carried out on a Mettler DSC 822 instrument at a scan rate of 10 K/min. Thermogravimetric analysis (TGA) was performed on a Perkin-Elmer TGA-7 thermal analysis system using dry nitrogen as a carrier gas at a flow rate of 40 mL/min. UV−Vis absorption and fluorescence spectra were obtained in specified solvents at room temperature using JASCO V-530 and Hitachi F-4500 spectrometers. IR spectra were obtained using a JASCO FT/IR-4100 spectrometer. Differential pulse voltammetry experiments were performed with a conventional three-electrode configuration (a platinum disk working electrode, an auxiliary platinum wire electrode, and a nonaqueous Ag reference electrode, with a supporting electrolyte of 0.1 M tetrabutylammonium hexafluorophosphate ($TBAPF_6$) in the specified dry solvent) using a CHI621C electrochemical analyzer (CH Instruments). All electrochemical potentials were referenced to an Fc^+/Fc internal standard (at +0.6 V). Elemental analyses were performed on a Heraeus CHN-O-Rapid elemental analyzer. Mass spectrometric data were obtained with a JMS-700 HRMS instrument. Benzo[d,d′]thieno[3,2-b;4,5-b′]-dithiophene (**BTDT**) and benzothiophenylbenzo[d,d′]thieno[3,2-b;4,5-b′]dithiophene (**BT-BTDT**; **2**) were prepared by one-pot [2 + 1 + 1] or traditional synthetic route as shown below.[11] Benzothieno-[3,2-b]thiophene,[12,13] and 2-bromorbenzothieno[3,2-*b*]thiophene[12] were prepared according to previous reports.

2.2. One-pot [2 + 1 + 1] Synthesis of Benzo[d,d′]thieno[3,2-b;4,5-b′]dithiophene (BTDT). Under nitrogen and anhydrous condition at −78 °C, 2.5 M *n*-BuLi (18.8 mL in hexanes, 0.047 mol) was slowly added to an ether solution (60 mL) of 3-bromobenzo[*b*]thiophene (10.0 g, 0.047 mol), and the mixture was stirred for 40 min. This solution was then warmed to 0 °C under vacuum to remove C_4H_9Br, then ether (200 mL) was added to the solution. At −78 °C, sulfur (1.65 g, 0.052 mol) was added to the ether solution, which was stirred for 30 min, warmed to 0 °C, and stirred for another 30 min. Next, p-toluenesulfonyl chloride (TsCl, 9.84 g, 0.052 mol) was added to this solution at 0 °C, stirred for 10 min, then the mixture was warmed to 45 °C for 4 h. 3-Li-thiophene was prepared as in the above procedure from 2.5 M *n*-BuLi (20.6 mL in hexanes, 0.052 mol) and 3-bromothiophene (5.0 mL, 0.052 mol). Again, this solution was warmed to 0 °C under vacuum to remove *n*-C_4H_9Br, and 30 mL of ether was added to the solution. At −78 °C, the 3-Li-thiophene portion of the ether solution was added to the first reaction mixture, stirred for 1 h, warmed to room temperature, and stirred overnight. At 0 °C, 2.5 M *n*-BuLi (42.6 mL in hexanes, 0.107 mol) was slowly added to the mixture, which was stirred for 30 min, and then refluxed for 2 h. Next, $CuCl_2$ (15.1 g, 0.113 mol) was added to the mixture at −78 °C, stirred for 10 min, warmed to room temperature, and stirred overnight. The resulting solids were collected by filtration, washed with water, extracted with benzene, and then chromatographed (silica gel; hexanes as the eluent). The **BTDT** product was recrystallized from hexanes as a light-yellow powder and was sublimed (130 °C, under vacuum) to give 4.6 g of white powder in a yield of 40%.

2.3. Synthesis of Benzo[d,d′]thieno[3,2-b;4,5-b′]dithiophene (BTDT) via Benzo[*d,d′*]thieno[3,2-*b*]thiophene (BTT); Method II. At 0 °C, NBS (1.02 g, 5.90 mmol) was added to a 50 mL THF solution of benzo[*d,d′*]thieno[3,2-*b*]thiophene (**BTT**) (1.0 g, 5.36 mmol), and the mixture was stirred for 30 min, warmed to room temperature, and stirred for 12 h. Next, $Na_2S_2O_3$ aqueous solution was added to this solution, and the desired product was extracted with ether and chromatographed (silica gel; hexanes as the eluent). 2-bromobenzo[*d,d′*]thieno[3,2-*b*]thiophene was further purified by recrystallization to give 1.3 g of white powder in a yield of 93%. ^{1}H NMR (300 MHz; acetone-d_6): δ 8.01 (m, J = 7.2 Hz, 1H), 7.94 (m, J = 7.2 Hz, 1H), 7.66 (s, 1H), 7.46 (m, 2H). Under nitrogen at 0 °C, 2-bromobenzo[*d,d′*]thieno[3,2-*b*]thiophene (12 g, 0.044 mol) was

dx.doi.org/10.1021/am3022448 | ACS Appl. Mater. Interfaces 2012, 4, 6992−6998

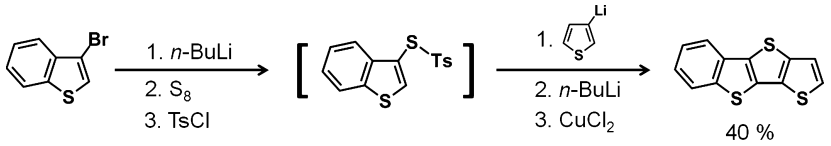

Figure 3. One-pot [2 + 1 + 1] synthesis of the **BTDT** semiconductor core.

added to a 200 mL THF solution of lithium diisopropylamine (LDA) (2.0 M, 44.6 mL, 0.088 mol), and the mixture was stirred for 1 h, then warmed to room temperature and stirred for 12 h. Next, water was added to this solution, THF was removed, and 3-bromobenzo[*d,d′*]thieno[3,2-*b*]thiophene was extracted with ether and chromatographed (silica gel; hexanes as the eluent). The product was further purified by recrystallization to give 7.2 g of white powder in a yield of 60%. ^{1}H NMR (300 MHz; $CDCl_3$): δ 7.90 − 7.82 (m, 2H), 7.47 − 7.37 (m, 2H), 7.395 (s, 1H). Under nitrogen at 0 °C, 3-bromobenzo[*d,d′*]thieno[3,2-*b*]thiophene (504 mg, 1.87 mmol) was added to a 30 mL THF solution of LDA (2 M, 1.4 mL, 2.8 mmol), and the mixture was stirred for 1 h at room temperature. At −78 °C, anhydrous *N*-formylpiperidine (0.31 mL, 2.80 mmol) was added to the mixture and was stirred at room temperature for 12 h. Dilute aqueous HCl was added to this solution and the organic precipitate, 3-bromobenzo[*d,d′*]thieno[3,2-*b*]thiophene-2-carbaldehyde, was collected by filtration and washed with hexanes to give 378 mg of brown solid in a yield of 68%. ^{1}H NMR (300 MHz; $CDCl_3$): δ 10.07 (s, 1H), 7.96 − 7.91 (m, 2H), 7.53 − 7.50 (m, 2H). Under nitrogen at 0 °C, ethyl 2-sulfanylacetate (0.36 mL, 3.24 mmol) was slowly added to a 100 mL DMF solution of 3-bromobenzo[*d,d′*]thieno[3,2-*b*]thiophene-2-carbaldehyde (642 mg, 2.16 mmol) and K_2CO_3 (627 mg, 4.53 mmol) and the mixture was stirred for 3 days at 60 °C. An aqueous solution of 6 M HCl was added to quench and neutralize the reaction and the organic precipitate, benzo[*d,d′*]thieno[3,2-*b*;4,5-*b′*]dithiophene-2-carboxylic acid ethyl ester, was collected by filtration and washed with hexanes to give 445 mg of brown solid in a yield of 65%. ^{1}H NMR (300 MHz; $CDCl_3$): δ 8.07 (s, 1H), 7.88 (t, J = 7.5 Hz, 2H), 7.49 − 7.39 (m, 2H), 4.41 (q, J = 7.2 Hz, 2H), 1.42 (t, J = 7.2 Hz, 3H). 10% NaOH aqueous solution (1.1 mL, 2.76 mmol) was added to a 50 mL THF solution of ethyl carboxylate-BTDT (251 mg, 0.79 mmol) and the mixture was refluxed for 12 h. THF was removed, 6 M HCl aqueous solution was added to the solution, and the organic precipitate, benzo[*d,d′*]thieno[3,2-*b*;4,5-*b′*]dithiophene-2-carboxylic acid, was collected by filtration, and was washed with water and CH_2Cl_2 to give 203 mg of brown powder in a yield of 89%. This material was insufficiently soluble to obtain useful ^{1}H and ^{13}C NMR spectra, and was used in the next step without further purification. Under nitrogen, a 100 mL quinoline solution of benzo[*d,d′*]thieno[3,2-*b*;4,5-*b′*]dithiophene-2-carboxylic acid (311 mg, 1.07 mmol) and Cu (68 mg, 1.07 mmol) was stirred at 250 °C for 12 h. After 6 M HCl was added to quench the reaction, Cu was filtered out and the organic fraction was extracted with CH_2Cl_2. The desired benzo[*d,d′*]thieno[3,2-*b*;4,5-*b′*]dithiophene was chromatographed (silica gel; hexanes as the eluent) and was further purified by recrystallization to give 120 mg of white powder in a yield of 46%.

2.4. Synthesis of 2-benzothieno[3,2-*b*]thiophenylbenzo[d,d′]thieno[3,2-b;4,5-b′]dithiophene (BTT-BTDT; 3). Under an anhyrdous nitrogen environment at 0 °C, 2.5 M *n*-BuLi (0.65 mL in hexanes, 1.64 mmol) was slowly added to a 30 mL THF solution of **BTDT** (403 mg, 1.64 mmol), and the mixture was stirred for 40 min. Next, tri-*n*-butyltin chloride (0.60 g, 1.80 mmol) was added to the solution and the mixture was stirred at 0 °C for 30 min, then warmed to room temperature and stirred for 8 h. After simple filtration under nitrogen, THF was removed under vacuum and 40 mL of toluene was loaded. This toluene solution was then transferred to a toluene (40 mL) solution of 2-bromobenzothieno[3,2-*b*]thiophene (485 mg, 1.80 mmol) and tetrakis(triphenylphosphine)palladium (76 mg, 0.06 mmol) and the mixture was refluxed at 140 °C for 2 days. After cooling back to room tempertaure, the mixture was filtered and washed with hexanes and subsequently ether, to give the crude product (582 mg) in a yield of 82%. The desired product was further purified by gradient sublimation at a pressure of ∼1 × 10^{-5} Torr at 275 − 300 °C (Mp: 349 °C). This material was insufficiently soluble to obtain useful ^{1}H and ^{13}C NMR spectra. Anal. Calcd for $C_{22}H_{10}S_5$: C, 60.79; H, 2.32. Found: C, 60.71; H, 2.40. HRMS (EI, *m/z*) calcd: 433.9386 (M^+). Found: 433.9388.

2.5. Synthesis of Bisbenzo[d,d′]thieno[3,2-b;4,5-b′]dithiophene (BBTDT; 4). Under nitrogen at 0 °C, 2.5 M *n*-BuLi (0.72 mL in hexanes, 1.79 mmol) was slowly added to a 30 mL THF solution of **BTDT** (441.8 mg, 1.79 mmol) and the mixture was stirred for 40 min. Next, tri-*n*-butyltin chloride (0.53 mL, 1.88 mmol) was added to the solution and the mixture was stirred at 0 °C for 30 min, then warmed to room temperature and stirred overnight. After simple filtration, THF was removed under vacuum and 30 mL of toluene was loaded. This toluene solution was then transferred to a toluene (50 mL) solution of 2-bromobenzo[d,d′]thieno[3,2-b;4,5-b′]dithiophene (612.5 mg, 1.97 mmol) and tetrakis(triphenylphosphine)palladium (83 mg, 0.07 mmol) and the mixture was refluxed for 2 days. The desired solid product was collected by filtration, washed with CH_2Cl_2 and then ether, and purified by gradient sublimation at pressures of ∼1 × 10^{-5} Torr, giving 391 mg of orange solid in a yield of 45%. This material was insufficiently soluble to obtain useful ^{1}H and ^{13}C NMR spectrum. Anal. Calcd for $C_{24}H_{10}S_6$: C, 58.74; H, 2.05. Found: C, 58.68; H, 2.11. HRMS (EI) *m/z*) calcd: 489.9102 (M^+). Found: 489.9107.

2.6. Device Fabrication and Characterization. For the fabrication of bottom-gate, bottom-contact OTFTs, metallic silver (100 nm) was deposited by sputtering onto a glass substrate as a bottom gate electrode, patterned by a shadow mask. Then, a 100 nm SiO_2 layer gate dielectric was thermally deposited onto the bottom gate electrode. For the OTS (octadecyltrichlorosilane) treatment, the SiO_2 surface was exposed to an OTS toluene solution in a self-assembly chamber for 10 h to give a hydrophobic surface with an advancing aqueous contact angle of ∼105°. A 100 nm-thick Au layer was thermally evaporated through a shadow mask to define source and drain contacts with a channel length and width of 100 and 500 μm, respectively. To reduce the contact resistance of the source/drain contacts to the semiconducting layer, the self-assembled monolayers (SAMs) were formed on source/drain contacts by immersing the patterned Au electrodes in a 20 mM ethanolic solution of n-octadecylthiol (Aldrich) for 1 h. The SAM-treated Au electrodes were then removed from the solution, rinsed with ethanol several times, and dried with N_2 gas. Subsequently, an organic semiconductor layer (50 nm) was thermally evaporated through a shadow mask onto the substrates which were held at predetermined temperatures of 30, 50, and 80 °C at a rate of 0.03 nm/s. All the vacuum deposition processes were conducted at a pressure of ∼1.6 × 10^{-6} Torr. Film thicknesses were measured using a Dektak 3030 profilometer. The capacitance of the gate insulators was measured using an HP 4284 A Precision LCR meter. The I−V characteristics of the fabricated OTFTs were measured in the dark with a semiconductor parameter analyzer (HP 4155A) for 10 different devices. All the films were examined by X-ray diffraction (XRD, Siemens D5000) with Cu Kα radiation. The surface morphology of all films was characterized using an atomic force microscope (AFM, Digital Instruments Nanoscope III).

3. RESULTS AND DISCUSSION

3.1. Synthesis. In our previous studies, we developed an efficient one-pot [1 + 1 + 2] synthetic route for the preparation of benzo[*d,d*]thieno[3,2-*b*;4,5-*b*]dithiophene (**BTDT**) core with an overall yield of 32%.[11] In this contribution, the newly designed one-pot [2 + 1 + 1] synthesis for a facile preparation

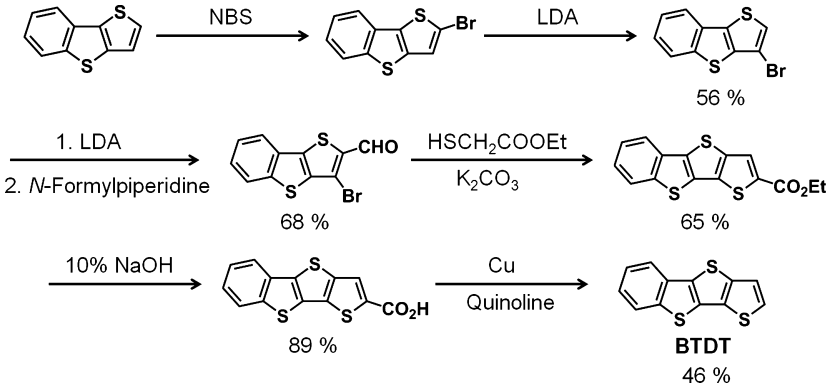

Figure 4. Other synthetic routes to **BTDT**.

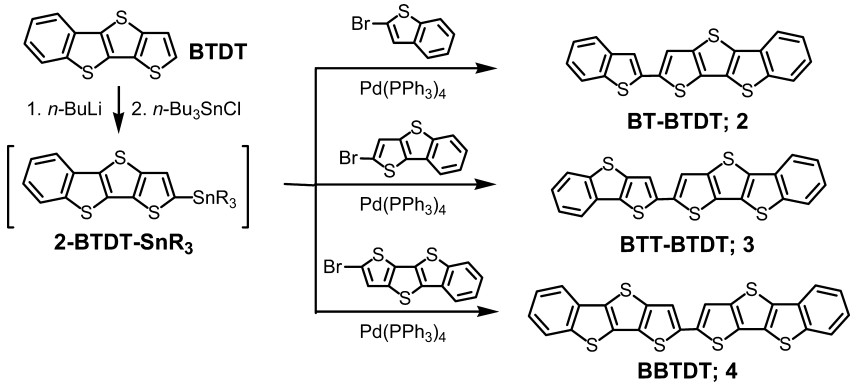

Figure 5. Synthetic routes to **BTDTs** (**2**–**4**).

Table 1. Thermal, Optical Absorption/Emission, and Electrochemical Data for BTDTs 1–4

compd	DSC T_m (°C)	TGA (°C; 5%)	UV–vis[a] λ_{max} (nm)	reductive potential (V)[b]	Oxidative potential(V)[b]	E_{gap} (eV) (UV)[a]	E_{gap} (eV) (DPV)[b]
2	341	309	378	−1.93	1.30	2.99	3.23
3	349	402	402	−1.91	1.14	2.83	3.05
4	461	471	412	−1.75	1.13	2.74	2.89

[a]In *o*-$C_6H_4Cl_2$. [b]By DPV in *o*-$C_6H_4Cl_2$ at 60 °C.

of **BTDT** was explored and the total yield was improved to 40%. As shown in Figure 3, 3-bromobenzo[*b*]thiophene was first lithiated with *n*-BuLi, followed by S_8 and subsequently TsCl addition. Next, the mixture was treated with 3-lithiumthiophene. Without product isolation, the crude mixture was dilithiated with *n*-BuLi and ring closure was achieved with $CuCl_2$ to afford **BTDT** with an overall yield of 40%. For comparison, this **BTDT** main core was also prepared via the synthetic route similar to that of dithieno[3,2-*b*:2A,3A-*d*]thiophene (**DTT**) preparation (Figure 4).[14] As shown, benzo[b]thieno[2,3-d]thiophene (BTT) was first brominated with NBS to give 2-bromobenzo[b]thieno[2,3-d]thiophene, which was subjected to halogen migration with LDA to give 3-bromobenzo[b]thieno[2,3-d]thiophene in a combined yield of 56%. Deprotonation of 3-bromobenzo[b]thieno[2,3-d]-thiophene with LDA and then direct formylation afforded 3-bromo-2-carbaldehyde benzo[b]thieno[2,3-d]thiophene in 68% yield. Annulations with ethyl mercaptoacetate in the presence of K_2CO_3 gave ethyl carboxylate benzo[*d*,*d*]thieno[3,2-*b*;4,5-*b*]dithiophene (65%), which was saponified and acidified, to form the corresponding carboxylic acid (89%). Finally, decarboxylation with copper in quinoline produced **BTDT** in a yield of 46%. Considering the laborious multistep procedures and much lower total yield (<10%) of the conventional synthetic method from benzo[*b*]thiophene, the newly developed one-pot [2 + 1 + 1] synthetic route demonstrated the most efficient way of asymmetric fused ring synthesis. Markedly, our one-pot synthetic route starts from inexpensive, commercially available materials and does not require expensive bis(phenyl-sulfonyl)sulfide, which is normally used in the previously reported fused thiophene synthesis.[15]

Following the synthesis of the **BTDT** core, functionalized **BTDTs** were synthesized as shown in Figure 5. For example, for the preparation of **BTT-BTDT** (**3**), **BTDT** was deprotonated with n-BuLi, and then alkylstannylated to generate BTDT-SnR_3 in situ. Next, the compound was coupled with the corresponding aryl bromide to produce the correspoding **BTDT** in ∼82% yield via the Stille coupling protocol. The resulting **BTDTs** were then further purified by gradient sublimation at a pressure of ∼1 × 10^{-5} Torr at 200–350 °C to give materials (in a yield of ∼50%) suitable for OTFT device fabrication.

3.2. Thermal and Optical Properties. For the **BTDT** derivatives, differential scanning calorimetry (DSC) scans

dx.doi.org/10.1021/am3022448 | ACS Appl. Mater. Interfaces 2012, 4, 6992–6998

exhibited sharp endotherms above 341 °C, and thermogravimetric analysis plots only showed weight loss (~5%) upon heating above 309 °C (Table 1), demonstrating excellent thermal stability of the developed compounds in this study among heteroacenes. In particular, **BTDT**-capped **BBTDT** (**4**) exhibited the highest melting point (461 °C) and the highest weight loss temperatures (471 °C) among the **BTDT** series. The optical absorption spectra of the compounds **BT-BTDT** (**2**; $\lambda_{max} \approx 378$ nm), **BTT-BTDT** (**3**; $\lambda_{max} \approx 402$ nm), and **BBTDT** (**4**; $\lambda_{max} \approx 412$ nm) are significantly red-shifted compared to that of phenyl-capped **P-BTDT** (**1**; $\lambda_{max} \approx 353$ nm) in *o*-$C_6H_4Cl_2$ solution (Figure 6). The HOMO−LUMO

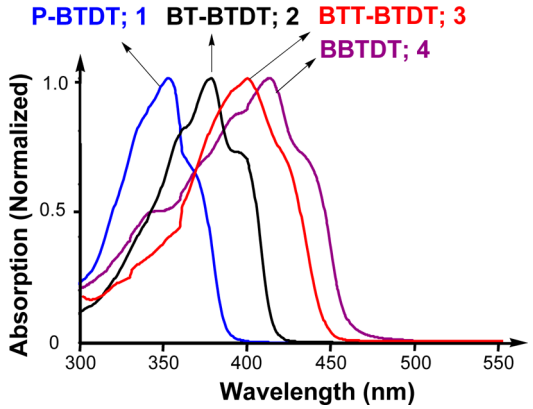

Figure 6. Optical spectra of **BTDT** derivatives in o-$C_6H_4Cl_2$ solution.

energy gaps calculated from the onset of the experimental optical absorption (2.74−2.99 eV) increase in the order **BBTDT** (**4**) < **BTT-BTDT** (**3**) < **BT-BTDT** (**2**), consistent with the electrochemically derived HOMO−LUMO gaps (*vide infra*). The greatest π-electron delocalization observed for the benzothienodithiophene substituted **BBTDT** (**4**) afforded the lowest HOMO−LUMO energy gap for the corresponding compound among the **BTDT** derivatives (Table 1).

Note that the HOMO−LUMO gaps of the **BTDT** series are significantly larger than that of pentacene (1.70−2.09 eV) or **ADT** derivatives (2.09−2.57 eV),[16] which suggests that **BTDT** derivatives are not easily oxidized and may have better stability in an ambient environment compared to pentacene and ADT derivatives. The photooxidative stability of the **BTDT** derivatives was examined by monitoring the absorbance decay at λ_{max} of the corresponding compounds in aerated *o*-$C_6H_4Cl_2$ solutions exposed to the white light of a fluorescent lamp at room temperature. Under these conditions, no decomposition was observed for all **BTDT**s after 5 days, demonstrating the good ambient stability of these materials.

3.3. Electrochemical Characterization. Differential pulse voltammograms (DPVs) of the **BTDT** derivatives were recorded in dichlorobenzene at 60 °C, and the resulting oxidation and reduction potentials are summarized in Table 1. The DPVs of the most conjugated **BBTDT** exhibited oxidation peaks around +1.13 V and reduction peaks at −1.75 V (using ferrocene/ferrocenium as an internal standard at +0.6 V). For comparison, the oxidation potential of less conjugated BT-BTDT (**2**; E_{ox} = +1.30 V) is shifted to more positive values and the reduction potential is shifted to more negative values (E_{red} = −1.93 V) compared to **BBTDT**, which can be attributed to the smaller molecular conjugation of the BT cap compared to BTDT. The electrochemically derived HOMO−LUMO energy gaps obtained from the DPV data are ranked in the order: **BBTDT** (2.89 eV) < **BTT-BTDT** (3.05 eV) < **BT-BTDT** (3.23 eV) (Figure 7; assuming ferrocene/ferrocenium oxidation

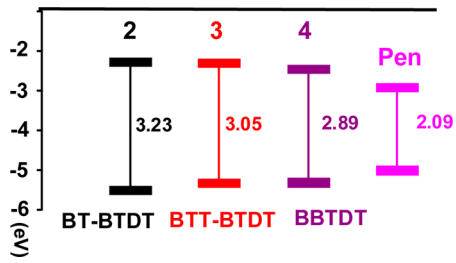

Figure 7. DPV-derived HOMO and LUMO energy levels of **BTDT**s (**2**−**4**) and pentacene (**Pen**).

at 4.8 eV), consistent with the values obtained from optical spectroscopy: **BBTDT** (2.74 eV) < **BTT-BTDT** (2.83 eV) < **BT-BTDT** (2.99 eV) (Table 1). The significantly lower HOMO energy level and the larger band gaps of the new **BTDT**s compared to pentacene suggest that these newly developed fused thiophenes are environmentally very stable (*vide supra*).

3.4. Thin-Film Transistor Characterization. Bottom-contact/bottom-gate OTFT devices were fabricated by the thermal evaporation of gold source and drain contacts (a channel length of 100 μm and width of 500 μm were used; gold contacts were treated with n-octadecylthiol before semiconductor deposition), followed by vacuum deposition (1.6×10^{-6} Torr) of each organic semiconductor on OTS-treated SiO_2/Ag (100 nm/100 nm) substrates at preset deposition temperatures (T_D values) of 30, 50, and 80 °C. The TFT properties were measured in an ambient environment to explore the device performance. All TFT data including carrier mobility, current on/off ratio, and threshold voltage are summarized in Table 2, and representative transfer and output plots are shown in Figures 8 (compound **4**) and S1 (compounds **2** and **3**).

Table 2. Carrier Mobilities (μ, cm^2/(V s)),[a] Current on/off Ratios (I_{on}/I_{off}), and Threshold Voltages (V_T, V) for OTFTs Fabricated by Vacuum Deposition of Compounds 2−4 at the Indicated Deposition Temperatures (T_D, °C)

compd	T_D (°C)	μ (cm^2/(V s))	I_{on}:I_{off}	V_T (V)
2	30	0.01	1×10^5	−2.2
	50	0.06	1×10^6	−3.1
	80	0.12	1×10^6	−1.2
3	30	0.01	1×10^6	−1.2
	50	0.07	1×10^7	−2.4
	80	0.18	1×10^7	−5.4
4	30	0.15	1×10^6	−4.8
	50	0.24	1×10^7	−4.1
	80	0.34	1×10^7	−3.8

[a]Device performance is an averaged value of at least 10 samples.

Devices fabricated with **BTDT** derivatives all exhibited TFT activity, performing as p-channel semiconductors. Among the compounds developed in this study, compound **4** (**BBTDT**), with the largest conjugation, exhibited the highest device performance with hole mobilities of 0.15−0.34 cm^2/(V s) and a current on/off ratio of 1×10^6 to 1×10^7 (Figure 8).[17]

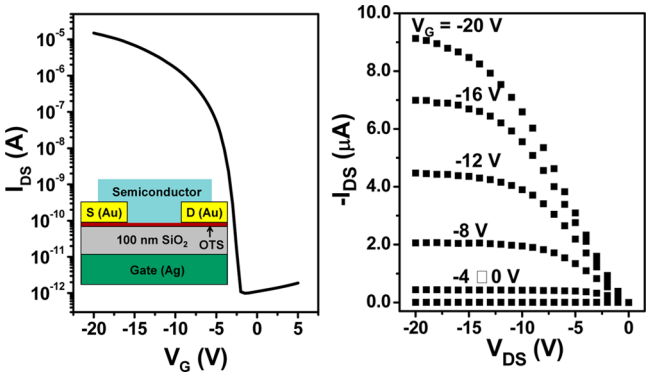

Figure 8. Transfer (V_{DS} = −16 V) and output plots of an OTFT device fabricated from **BBTDT** (**4**) films grown on an OTS-coated SiO_2 substrate (T_D = 80 °C, channel length = 100 μm, channel width = 500 μm). (Inset) The OTFT device structure employed in this study.

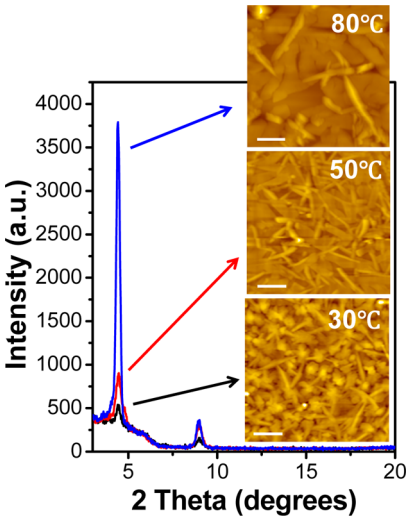

Figure 9. θ–2θ XRD scans (black, T_D = 30 °C; red, T_D = 50 °C; blue, T_D = 80 °C) and AFM images (5 × 5 μm²) of **BBTDT** (**4**) films vapor-deposited at the indicated value of T_D on OTS-coated SiO_2 substrates (scale bars indicate 1 μm).

Compounds **2** and **3** showed lower device performance than compound **4** with carrier mobilities of 0.01−0.12 $cm^2/(V\ s)$ and 0.01−0.18 $cm^2/(V\ s)$, respectively. Current on/off ratios of compounds **2** and **3** were comparable to that of compound **4**. Derived carrier mobilities of the **BTDT** derivatives depended strongly upon the deposition temperature (T_D). In the range of T_D = 30−80 °C, enhanced device performance was observed at higher deposition temperatures. A clear correlation between μ and T_D was also evident in the XRD and AFM characterization data of the corresponding semiconductor films (vide infra).

3.5. Thin-Film Microstructure and Morphology. Film microstructure (crystallinity) and surface morphology of vacuum-deposited films are often used to evaluate device performance. Generally, films with high crystallinity and large grain size with excellent grain interconnectivity exhibit high device performance, and hence, high carrier mobilities.[4] Therefore, thin-film microstructures and morphologies of **BTDT** derivatives were studied using wide-angle θ-2θ XRD and AFM. Conventional θ/2θ XRD scans were utilized to obtain out-of-plane *d*-spacings in the vacuum-deposited thin films on OTS-coated SiO_2 substrates at various values of T_D. The thicknesses of all films were ∼50 nm, as measured by profilometry. Representative XRD scans of the thin films of **BTDT** derivatives are shown in Figures 9 (compound **4**) and S2 (compounds **2** and **3**).

The θ/2θ XRD scan of **BBTDT** (**4**) films (Figure 9) indicated highly textured films having high peak intensities among **BTDT** series, consistent with the highest TFT performance, as described above. The first reflection in the XRD spectrum was observed at 2θ = 4.43°, corresponding to a *d*-spacing of 19.9 Å, comparable to the molecular length (∼20.6 Å) of the compound.[18] This indicates that the films could be predominantly aligned with their long molecular axes along the substrate normal. Films of **BTT-BTDT** (**3**) and **BT-BTDT** (**2**) with decent carrier mobility (but lower than **BBTDT**) showed a similar XRD pattern with slightly lower peak intensities, when compared to **BBTDT** (see Figure S2A in the Supporting Information). Low film texturing of compounds **2** and **3** is possibly due to smaller molecular conjugation of the corresponding molecules compared to **BBTDT**. The *d*-spacings of the **BTT-BTDT** and **BT-BTDT** films (observed at 2θ = 4.90 and 5.60° for the first reflections) were 18.0 Å and 17.0 Å, respectively.[19] Because the TFT performance was sensitive to the deposition temperature (*vide supra*), T_D-dependent XRD patterns were also examined. There is a clear correlation between mobility values and XRD peak intensity. As the T_D increases, the XRD peak intensity for films (with the same thickness of ∼50 nm) of all compounds increases and sharpens (Figure 9 and Figure S2 in the Supporting Information), as does the TFT carrier mobility (*vide supra*).

Charge transport in OTFT is confined to a thin semiconducting region at the semiconductor/dielectric interface. It is very difficult, however, to characterize the dielectric-semiconductor interface using conventional experimental techniques. Hence, surface morphologies of organic semiconductor thin films (50 nm), which contain information about the underlying microstructure at the semiconductor/dielectric interface, were characterizaed by AFM (Figure 9 and Figure S3 in the Supporting Information). As shown, films of **BBTDT** showed faceted and rod-like grain morphologies, while **BT-BTDT** and **BTT-BTDT** exhibited ball-shaped grains. Furthermore, similar to the XRD patterns, surface morphologies of the films also displayed a strong dependence on T_D, and a correlation with the device performance (vide supra). All films of **BTDT** derivatives in this study exhibited larger grain sizes at higher deposition temperatures, which correlates well with the enhanced TFT performance.

4. CONCLUSIONS

A family of new benzo[d,d′]thieno[3,2-b;4,5-b′]dithiophenes-based semiconductors was synthesized and characterized. Bottom-gate/bottom-contact thin-film transistors fabricated from these molecules exhibited excellent device performance with decent air stability. Films deposited on OTS-coated SiO_2 substrates under properly adjusted substrate temperature afforded high film crystallinity and good film grain interconnectivity, resulting in high OTFT performance, with a mobility as high as 0.34 $cm^2/(V\ s)$ and a current on/off ratio as high as 1 × 10^7.

■ ASSOCIATED CONTENT

Supporting Information

OTFT device performance, XRD data, and AFM data. This material is available free of charge via the Internet at http://pubs.acs.org.

■ AUTHOR INFORMATION

Corresponding Author

*E-mail: mcchen@ncu.edu.tw (M.-C-C.); (choongik@sogang.ac.kr (C.K.).

Author Contributions

‡These authors contributed equally to this work.

Notes

The authors declare no competing financial interest.

■ ACKNOWLEDGMENTS

This work was supported by the National Science Council, Taiwan, Republic of China (Grants NSC100-2628-M-008-004 and NSC100-2627-E-006-001), Industrial Technology Research Institute of Taiwan, by the National Research Foundation of Korea (2011-0007730), by a grant (2011-0031628) from the Center for Advanced Soft Electronics under the Global Frontier Research Program of the Ministry of Education, Science and Technology, Korea, and by the Human Resources Development of the Korea Institute of Energy Technology Evaluation and Planning (KETEP) grant funded by the Korea government Ministry of Knowledge Economy (20114010203090).

■ REFERENCES

(1) (a) Forrest, S. R. *Nature* **2004**, *428*, 911. (b) Murphy, A. R.; Frechet, J. M. J. *Chem. Rev.* **2007**, *107*, 1066. (c) Usta, H.; Facchetti, A.; Marks, T. J. *Acc. Chem. Res.* **2011**, *44*, 501. (d) Anthony, J. E. *Chem. Rev.* **2006**, *106*, 5028. (e) Yan, H.; Chen, Z. H.; Zheng, Y.; Newman, C.; Quinn, J. R.; Dotz, F.; Kastler, M.; Facchetti, A. *Nature* **2009**, *457*, 679. (f) Tang, M. L.; Mannsfeld, S. C. B.; Sun, Y. S.; Becerril, H. A.; Bao, Z. *J. Am. Chem. Soc.* **2009**, *131*, 882.

(2) (a) Marrocchi, A.; Seri, M.; Kim, C.; Facchetti, A.; Taticchi, A.; Marks, T. J. *Chem. Mater.* **2009**, *21*, 2592. (b) Didane, Y.; Mehl, G. H.; Kumagai, A.; Yoshimoto, N.; Videlot-Ackermann, C.; Brisset, H. *J. Am. Chem. Soc.* **2008**, *130*, 17681. (c) Subramanian, S.; Park, S. K.; Parkin, S. R.; Podzorov, V.; Jackson, T. N.; Anthony, J. E. *J. Am. Chem. Soc.* **2008**, *130*, 2706. (d) Ashizawa, M.; Yamada, K.; Fukaya, A.; Kato, R.; Hara, K.; Takeya, J. *Chem. Mater.* **2008**, *20*, 4883. (e) Yagodkin, E.; Xia, Y.; Kalihari, V.; Frisbie, C. D.; Douglas, C. J. *J. Phys. Chem. C* **2009**, *113*, 16544. (f) Ortiz, R. P.; Casado, J.; Hernandez, V.; Navarrete, J. T. L.; Letizia, J. A.; Ratner, M. A.; Facchetti, A.; Marks, T. J. *Chem.—Eur. J.* **2009**, *15*, 5023. (g) Osaka, I.; Abe, T.; Shinamura, S.; Miyazaki, E.; Takimiya, K. *J. Am. Chem. Soc.* **2010**, *132*, 5000.

(3) (a) Facchetti, A. *Mater. Today* **2007**, *10*, 28. (b) Arias, A. C.; Mackenzie, J. D.; McCulloch, I.; Rivnay, J.; Salleo, A. *Chem. Rev.* **2010**, *110*, 3.

(4) (a) Kim, C.; Facchetti, A.; Marks, T. J. *Science* **2007**, *318*, 76. (b) Newman, C. R.; Frisbie, C. D.; da Silva, D. A.; Filho, S.; Brédas, J.-L.; Ewbank, P. C.; Mann, K. R. *Chem. Mater.* **2004**, *16*, 4436.

(5) (a) Marks, T. J. *MRS Bull.* **2010**, *35*, 1018. (b) Minuti, L.; Taticchi, A.; Marrocchi, A.; Landi, S.; Gacs-Baitz, E. *Tetrahedron Lett.* **2005**, *46*, 5735. (c) Wolfer, P.; Santarelli, M. L.; Vaccaro, L.; Yu, L.; Anthopoulos, T. D.; Smith, P.; Stingelin, N.; Marrocchi, A. *Org. Electron.* **2011**, *12*, 1886. (d) Facchetti, A.; Vaccaro, L.; Marrocchi, A. *Angew. Chem., Int. Ed.* **2012**, *51*, 3520.

(6) (aa) Kelley, T. W.; Boardman, L. D.; Dunbar, T. D.; Muyres, D. V.; Pellerite, M. J.; Smith, T. Y. P. *J. Phys. Chem. B* **2003**, *107*, 5877. (bb) Klauk, H.; Halik, M.; Zschieschang, U.; Eder, F.; Schmid, G.; Dehm, C. *Appl. Phys. Lett.* **2003**, *82*, 4175. (a) Gao, J. H.; Li, R. J.; Li, L. Q.; Meng, Q.; Jiang, H.; Li, H. X.; Hu, W. P. *Adv. Mater.* **2007**, *19*, 3008. (b) Yamada, H.; Yamashita, Y.; Kikuchi, M.; Watanabe, H.; Okujima, T.; Uno, H.; Ogawa, T.; Ohara, K.; Ono, N. *Chem.—Eur. J.* **2005**, *11*, 6212. (c) Maliakal, A.; Raghavachari, K.; Katz, H. E.; Chandross, E.; Siegrist, T. *Chem. Mater.* **2004**, *16*, 4980. (d) Coppo, P.; Yeates, S. G. *Adv. Mater.* **2005**, *17*, 3001. (e) Meng, H.; Bendikov, M.; Mitchell, G.; Helgeson, R.; Wudl, F.; Bao, Z.; Siegrist, T.; Kloc, C.; Chen, C. H. *Adv. Mater.* **2003**, *15*, 1090.

(7) (a) Sun, Y. M.; Ma, Y. W.; Liu, Y. Q.; Lin, Y. Y.; Wang, Z. Y.; Wang, Y.; Di, C. G.; Xiao, K.; Chen, X. M.; Qiu, W. F.; Zhang, B.; Yu, G.; Hu, W. P.; Zhu, D. B. *Adv. Funct. Mater.* **2006**, *16*, 426. (b) Tan, L.; Zhang, L.; Jiang, X.; Yang, X. D.; Wang, L. J.; Wang, Z.; Li, L. Q.; Hu, W. P.; Shuai, Z. G.; Li, L.; Zhu, D. B. *Adv. Funct. Mater.* **2009**, *19*, 272. (c) Liu, Y.; Di, C. A.; Du, C. Y.; Liu, Y. Q.; Lu, K.; Qiu, W. F.; Yu, G. *Chem.—Eur. J.* **2010**, *16*, 2231.

(8) (a) Liu, Y.; Wang, W.; Wu, Y.; Liu, H.; Xi, L.; Wang, W.; Qui, K.; Lu, C. Du; Yu, G. *Adv. Funct. Mater.* **2009**, *19*, 772. (b) Gao, J.; Li, R.; Li, L.; Meng, Q.; Jiang, H.; Li, H.; Hu, W. *Adv. Mater.* **2007**, *19*, 3008.

(9) (a) Ebata, H.; Izawa, T.; Miyazaki, E.; Takimiya, K.; Ikeda, M.; Kuwabara, H.; Yui, T. *J. Am. Chem. Soc.* **2007**, *129*, 15732. (b) Takimiya, K.; Ebata, H.; Sakamoto, K.; Izawa, T.; Otsubo, T.; Kunugi, Y. *J. Am. Chem. Soc.* **2006**, *128*, 12604. (c) Takimiya, K.; Kunugi, Y.; Konda, Y.; Ebata, H.; Toyoshima, Y.; Otsubo, T. *J. Am. Chem. Soc.* **2006**, *128*, 3044. (d) Takimiya, K.; Kunugi, Y.; Konda, Y.; Niihara, N.; Otsubo, T. *J. Am. Chem. Soc.* **2004**, *126*, 5084.

(10) (a) Chen, M.-C.; Chiang, Y.-J.; Kim, C.; Guo, Y.-J.; Chen, S.-Y.; Liang, Y.-J.; Huang, Y.-W.; Hu, T.-S.; Lee, G.-H.; Facchetti, A.; Marks, T. J. *Chem. Commun.* **2009**, *14*, 1846. (b) Kim, C.; Chen, M.-C.; Chiang, Y.-J.; Guo, Y.-J.; Youn, J.; Huang, H.; Liang, Y.-J.; Lin, Y.-J.; Huang, Y.-W.; Hu, T.-S.; Lee, G.-H.; Facchetti, A.; Marks, T. J. *Org. Electron.* **2010**, *11*, 801. (c) Youn, J.; Huang, P.-Y.; Huang, Y.-W.; Chen, M.-C.; Lin, Y.-J.; Huang, H.; Ortiz, R. P.; Stern, C.; Chung, M.-C.; Feng, C.-Y.; Chen, L.-H.; Facchetti, A.; Marks, T. J. *Adv. Funct. Mater.* **2012**, *22*, 48.

(11) Youn, J.; Chen, M.-C.; Liang, Y.-J.; Huang, H.; Ortiz, R. P.; Kim, C.; Stern, C.; Hu, T.-S.; Chen, L.-H.; Yan, J.-Y.; Facchetti, A.; Marks, T. J. *Chem. Mater.* **2010**, *22*, 5031.

(12) Chen, H.; Cui, Q.; Yu, G.; Guo, Y.; Huang, J.; Zhu, M.; Guo, X.; Liu, Y. *J. Phys. Chem. C* **2011**, *115*, 23984.

(13) (a) Fouad, I.; Mechbal, Z.; Chane-Ching, K. I.; Adenier, A.; Maurel, F.; Aaron, J.-J.; Vodicka, P.; Cernovska, K.; Kozmik, V.; Svoboda, J. *J. Mater. Chem.* **2004**, *14*, 1711. (b) Balenko, S. K.; Makarova, N. I.; Karamov, O. G.; Rybalkin, V. P.; Dorogan, I. V.; Popova, L. L.; Shepelenko, E. N.; Metelitsa, A. V.; Tkachev, V. V.; Aldoshin, S. M.; Bren, V. A.; Minkin, V. I. *Russ. Chem. Bull.* **2007**, *56*, 2400. (c) Ricci, A.; Balucani, D.; Bettelli, M. *Gaz. Chim. Ital.* **1971**, *101*, 774.

(14) Frey, J.; Bond, A. D.; Holmes, A. B. *Chem. Commun.* **2002**, 2424.

(15) (a) Zhang, X. N.; Cote, A. P.; Matzger, A. J. *J. Am. Chem. Soc.* **2005**, *127*, 10502. (b) Allared, F.; Hellberg, J.; Remonen, T. *Tetrahedron Lett.* **2002**, *43*, 1553. (c) Mazaki, Y.; Kobayashi, K. *Tetrahedron Lett.* **1989**, *30*, 3315.

(16) (a) Kim, C.; Huang, P.-Y.; Jhuang, J.-W.; Chen, M.-C.; Ho, J.-C.; Hu, T.-S.; Yan, J.-Y.; Chen, L.-H.; Lee, G.-H.; Facchetti, A.; Marks, T. J. *Org. Electron.* **2010**, *11*, 1363. (b) Chen, M.-C.; Kim, C.; Chen, S.-Y.; Chiang, Y.-J.; Chung, M.-C.; Facchetti, A.; Marks, T. J. *J. Mater. Chem.* **2008**, *18*, 1029.

(17) OTFT device based on compound **4** (T_D of 80 °C) showed decent performance after two month stored in an ambient environment with mobility of 0.1 $cm^2/(V\ s)$, current on/off ratio of 1×10^5, and threshold voltage of 1.5 V.

(18) Molecular length of the compounds was estimated from Chem3D software after energy minimization.

(19) The *d*-spacings of the BTDT derivatives employed in this study were in the order: BT-BTDT < BTT-BTDT < BBTDT, which is consistent with the molecular length of the corresponding compound.